University of Massachusetts Amherst

ScholarWorks@UMass Amherst

2004

A Study of CO Emission in High-Redshift QSOs Using the Owens Valley Millimeter Array

LJ Hainline

NZ Scoville

Min Yun
University of Massachusetts - Amherst

DW Hawkins

DT Frayer

See next page for additional authors

Recommended Citation

Hainline, LJ; Scoville, NZ; Yun, Min; Hawkins, DW; Frayer, DT; and Isaak, KG, "A Study of CO Emission in High-Redshift QSOs Using the Owens Valley Millimeter Array" (2004). *Astronomy Department Faculty Publication Series*. 1106.
10.1086/420920

Authors

LJ Hainline, NZ Scoville, Min Yun, DW Hawkins, DT Frayer, and KG Isaak

A Study of CO Emission in High Redshift QSOs Using the Owens Valley Millimeter Array

Laura J. Hainline and N. Z. Scoville

Dept. of Astronomy, California Institute of Technology, Mail Code 105-24, Pasadena, CA 91125, USA

ljh@astro.caltech.edu, nzs@astro.caltech.edu

Min S. Yun

Dept. of Physics and Astronomy, University of Massachusetts, Amherst, MA 01003, USA

myun@astro.umass.edu

D. W. Hawkins

Owens Valley Radio Observatory, California Institute of Technology, Big Pine, CA 93513, USA

dwh@ovro.caltech.edu

D. T. Frayer

Spitzer Science Center, California Institute of Technology, Mail Code 220-06, Pasadena, CA 91125, USA

frayer@ipac.caltech.edu

and

Kate G. Isaak

Department of Physics and Astronomy, Cardiff University, 5 The Parade, Cardiff CF24 3YB UK

kate.isaak@astro.cf.ac.uk

ABSTRACT

Searches for CO emission in high-redshift objects have traditionally suffered from the accuracy of optically-derived redshifts due to lack of bandwidth

in correlators at radio observatories. This problem has motivated the creation of the new COBRA continuum correlator, with 4 GHz available bandwidth, at the Owens Valley Radio Observatory Millimeter Array. Presented here are the first scientific results from COBRA. We report detections of redshifted $CO(J = 3 \rightarrow 2)$ emission in the QSOs SMM J04135+10277 and VCV J140955.5+562827, as well as a probable detection in RX J0911.4+0551. At redshifts of $z = 2.846$, $z = 2.585$, and $z = 2.796$, we find integrated CO flux densities of 5.4 Jy km s^{-1}, 2.4 Jy km s^{-1}, and 2.9 Jy km s^{-1} for SMM J04135+10277, VCV J140955.5+562827, and RX J0911.4+0551, respectively, over linewidths of $\Delta V_{FWHM} \sim 350$ km s^{-1}. These measurements, when corrected for gravitational lensing, correspond to molecular gas masses of order $M(H_2) \sim 10^{9.6-11.1} \, M_\odot$, and are consistent with previous CO observations of high-redshift QSOs. We also report 3σ upper limits on CO(3→2) emission in the QSO LBQS 0018-0220 of 1.3 Jy km s^{-1}. We do not detect significant 3 mm continuum emission from any of the QSOs, with the exception of a tentative (3σ) detection in RX J0911.4+0551 of $S_{3mm} = 0.92$ mJy beam^{-1}.

Subject headings: galaxies: active — galaxies: formation — galaxies: evolution — radio lines: galaxies

1. INTRODUCTION

High-redshift QSOs have been shown to be often associated with dusty host galaxies (e.g. Barvainis & Ivison 2002b), and as such offer much potential as powerful probes of the formation and evolution of massive galaxies in the universe. The masses of high-redshift host galaxies, as inferred by extrapolation from the locally measured correlation between central, supermassive QSO black hole masses and the velocity dispersion of stars in the host galaxy spheroids (Gebhardt et al. 2000; Ferrarese & Merritt 2000) are large. Thus, high-redshift QSOs are signposts to the position and redshift of massive galaxies in the early universe. Many high-redshift QSOs have been detected by recent millimeter and submillimeter surveys (e.g. Carilli et al. 2001; Isaak et al. 2002; Barvainis & Ivison 2002b), implying that there is a link between QSOs and the massive, dusty, and gas-rich galaxy population discovered by deep submillimeter surveys (e.g. Smail, Ivison, & Blain 1997; Cowie, Barger, & Kneib 2002). Most of these so-called submillimeter sources are too faint for optical redshifts to be determined, even with the largest telescopes, precluding deep searches for the large molecular gas reservoirs associated with young, massive galaxies. By studying large samples of dusty, high-z QSOs and the gas and dust properties of their host systems, we can evaluate

their overlap with the submillimeter galaxy population and investigate their properties and evolution.

Recently, studies of CO emission in high-redshift objects have seen much success, with over 20 separate galaxies detected (e.g. Barvainis, Alloin, & Bremer 2002a; Guilloteau et al. 1999), the majority from galaxies with $S_{850\mu m} > 10$ mJy (e.g. Figure 1 in Isaak et al. 2002). From these measurements it is possible to infer the total molecular gas mass in the high-z host galaxies, and in turn establish the fraction of the total mass that is still in gaseous form – a suggestive indicator of evolutionary state.

CO measurements also provide long-sought evidence of previous metal enrichment, both in these objects and in the early universe, since carbon and oxygen are mainly produced by fusion reactions in stellar cores. These stars must also have produced copious amounts of other heavy elements. We therefore expect to see metal-rich gas ($Z \sim Z_\odot$) in massive starbursting systems very soon after the first starbursts (after ~ 200 Myr). The spectacular detections of both CO (Walter et al. 2003; Bertoldi et al. 2003b) and inferred presence of dust (Bertoldi et al. 2003a; Robson et al. 2004) in SDSS 1148+5251 indicate that heavy-element enriched gas was already present in some objects at $z = 6.4$, within 800 Myr of the Big Bang. Star formation must have already been an important process by $z \sim 6.4$. The growing number of CO detections at lower, yet still cosmologically significant, redshifts, are very important, indicating how widespread star forming systems were at early epochs, and supporting the link between submillimeter galaxies and QSO hosts.

Searches for high-redshift CO have been hampered by the limited spectrometer band-widths (typically about 500-1500 km s^{-1}) available to date on the current generation of millimeter telescopes and interferometers. The lack of bandwidth prevents easy search for CO emission because the optically-determined redshifts for QSOs, typically measured from broad emission lines, are known to be blueshifted from the host galaxy redshifts by as much as 1000-2000 km s^{-1} (Tytler & Fan 1992). As an example, the QSO APM 08279+5255 has an optical redshift of $z = 3.87$ from Irwin et al. (1998), determined through identification of its rest-frame UV emission lines; by contrast, the redshift of the CO line of its host galaxy, from Downes et al. (1999), is $z_{CO} = 3.911$, a discrepancy of approximately 2500 km s^{-1} (blueshifted). At the Owens Valley Radio Observatory (OVRO), a new very broadband cross-correlator system, named COBRA, has been recently implemented to alleviate this problem. With a spectral coverage of 4 GHz, COBRA represents an eight-fold increase over the previous bandwidth at OVRO, and currently provides the largest available bandwidth for CO searches at millimeter wavelengths. This system is particularly advantageous for high-redshift spectral line searches when the redshift is poorly known *a priori*. Presented in Figure 1 is a sample COBRA spectrum, showing 3 GHz of the 4 GHz available bandwidth.

As part of the correlator commissioning, we started a program to detect CO emission from high-redshift QSOs. To this end, we compiled a database of submillimeter-bright, $z > 2$ QSOs from the literature from which to choose a sample of targets. To be included in the list, each object was required to meet the following criteria: (1) detection in 2 or more submillimeter/far-infrared (FIR) bands; (2) $T_{dust} \leq 100$ K, as derived following Yun & Carilli (2002), such that the rest-FIR spectral energy distribution includes a significant cold dust contribution; and (3) FIR luminosity greater than or equal to that of the prototypical ULIRG Arp 220 (i.e. $L_{FIR} > 10^{12.2} L_\odot$). We chose a total of 4 QSOs from the total of 23 sources in this database to observe, selecting those with the greatest FIR luminosities but without a published CO detection: LBQS 0018-0220, SMM J04135+10277, RX J0911.4+0551, and VCV J140955.5+562827. In the sections that follow, we detail our observations and report the results of our efforts, which are part of an ongoing program of observations at OVRO.

Throughout this paper, we assume an $\Omega_M = 0.3$, $\Omega_\Lambda = 0.7$ cosmology with $H_0 = 70$ km s^{-1} Mpc^{-1}. We also provide a parallel analysis in parentheses in the Einstein-deSitter cosmology $\Omega_M = 1$ and $\Omega_\Lambda = 0$, with $H_0 = 75$ km s^{-1} Mpc^{-1}.

2. OBSERVATIONS AND DATA CALIBRATION

A search for redshifted CO(3→2) ($\nu_{rest} = 345.796$ GHz) emission from the submillimeter-bright QSOs listed in Table 1 was made during 2003 May - June with the OVRO Millimeter Array in the compact (C) configuration [1] and the new COBRA correlator. This is the lowest resolution configuration of the six 10.4-m telescopes, and is that most sensitive for searches for millimeter emission from high-redshift sources. Listed in Table 1 are the observational parameters for each source. The redshifts have been taken from the published broad optical emission line redshifts with an offset applied in an attempt to correct for possible emission-line bias in the optical redshift, because previous searches near the broad-line redshift of some QSOs have failed. Typical single-sideband temperatures in the frequency range 87-99 GHz were between 200-400 K, corrected for antenna and atmospheric losses. The weather during the observations was good, especially for the time of year, and poor phase coherence was rarely a problem.

The new COBRA digital cross-correlator provides 4 GHz of instantaneous bandwidth in each receiver sideband with 8 32-channel spectrometers (each with 500 MHz BW). The correlator is based on FPGA chips operating at clock speeds of 125 MHz (Hawkins et al. in preparation). At $\lambda \simeq 3$ mm, each 15.625 MHz-width channel corresponds to ~ 50 km s^{-1} and

---

[1] In this configuration, the interferometer has baselines ranging in length between 18 and 55 meters.

so the full velocity coverage is 12,000 km s^{-1} (c.f. galaxy CO linewidths, 100-1000 km s^{-1}, velocity separations of interacting galaxies, $\lesssim$ 500 km s^{-1}, and galaxy cluster velocity dispersions, $\lesssim$ 1000 km s^{-1}). For each observation, COBRA was centered in the lower side-band at the frequency listed for each source in Table 1. In addition, 3 mm continuum data were recorded simultaneously with the older, 2 GHz bandwidth analog continuum correlator at OVRO.

Nearby radio-loud quasars listed in Table 1 for each source were observed every 20 minutes for passband, gain, and phase calibration. Absolute flux calibration was determined from observations of various combinations of 3C 273, 3C 84, 3C 345, and 3C 454.3, the flux histories of which are monitored by observations of Uranus and Neptune. The absolute flux calibration uncertainty for the data is within 15% for each source. The total integration time and spatial resolution for each source varied with system scheduling, source declination, and observed frequency, and is listed in Table 1.

The data were reduced using the latest version of the OVRO MMA software (Scoville et al. 1993), updated for use with COBRA data. Data mapping was accomplished using standard tasks in MIRIAD (Sault, Teuben, & Wright 1995).

3. RESULTS AND DISCUSSION

3.1. New Detections

3.1.1. SMM J04135+10277

SMM J04135+10277, located behind the galaxy cluster Abell 478 ($z = 0.088$), is the first type-1 QSO to have been discovered by nature of its submillimeter emission. It was found in the Leiden-SCUBA Lensed Survey (Knudsen, van der Werf, & Jaffe 2003) which is a survey of several galaxy cluster fields designed to detect gravitationally amplified, background submillimeter sources with the SCUBA instrument (Holland et al. 1999) on the James Clerk Maxwell Telescope. One of the brightest submillimeter sources known, its fluxes measured with SCUBA are $S_{850\mu m} = 25 \pm 2.8$ mJy and $S_{450\mu m} = 55 \pm 17$ mJy. The first optical-wavelength study of this QSO was recently published in Knudsen et al. (2003), in which a spectroscopic redshift of $z = 2.837 \pm 0.003$ from broad emission lines as well as $I = 20.5$ (not corrected for Galactic extinction; $I = 19.4$ when a reddening of $E(B-V) = 0.52$ is taken into account) were measured. The I-band source was found to be located $\sim 2''$ southeast

of the SCUBA position for SMM J04135+10277, within the source's SCUBA error circle[2]. The authors attribute the optical faintness of this QSO to a large viewing angle from the direction of relativistic beaming. A gravitational lensing analysis by Knudsen et al. (2003) using LENSTOOL (Kneib et al. 1993) yields a magnification factor of 1.3. The same authors, in an analysis of the galaxy's infrared (IR) SED (shown in Figure 3 of Knudsen et al. 2003), find $T_{dust} = 29$ K, but say they cannot determine the temperature of the hot dust (due to the AGN) because of gaps in the IR SED. Furthermore, the quasar is considered to be radio-quiet based on archived NVSS data, having a 3σ upper limit of 1.5 mJy at 1.4 GHz (Condon et al. 1998).

A moment map of integrated CO(3→2) emission for SMM J04135+10277 is shown in Figure 2a. No other significant CO sources at the same redshift are seen within the telescope's main beam, $\sim 70''$. Obtaining the value of σ for the map from the median single-channel rms per pixel over the 64 pixel $\times$ 64 pixel map, excluding the 5 edge pixels on each side of the map, the peak of emission is detected at a significance level of 5.4σ at 89.911 GHz, corresponding to a redshift of $z_{CO} = 2.846 \pm 0.002$. We calculate the uncertainty in the redshift according to the formula

$$\sigma_z = (\nu_{rest}/\nu_{obs}^2)(\Delta\nu_{obs}) \tag{1}$$

where ν_{rest} is the rest frequency of the line, ν_{obs} is the frequency at which the line is observed, and $\Delta\nu_{obs}$ is the uncertainty in the center position of the line. The value of z_{CO} lies slightly outside the stated error range of the broad-line redshift reported in Knudsen et al. (2003). The discrepancy, $\Delta z = 0.009$ or $\Delta v \sim +700$ km s^{-1}, is not surprising, and is in fact less than the correction we applied to the optical redshift ($\Delta z = 0.018$) to search for CO. By fitting a two-dimensional Gaussian profile directly to the emission map in the image plane, we find an upper limit to the source size of $14''.0 \times 7''.0$. The low resolution and low signal-to-noise (S/N) of our observations prevents us from determining any meaningful morphology of the QSO host from the map. No 3 mm continuum emission was detected from SMM J04135+10277 using data from the 2 GHz bandwidth analog continuum correlator at OVRO, with a 3σ upper limit of $S_{3mm} < 0.9$ mJy beam^{-1}.

In Figure 2a it can be seen that the peak CO emission from SMM J04135+10277 is offset by several arcseconds to the northwest from the pointing (phase) center of the observation. The coordinates published by Knudsen et al. (2003) ($\alpha_{J2000} = 04^h13^m27^s.28$, $\delta_{J2000} = +10°27'41''.4$) explain this offset: they indicate that the position we observed was too far to the east. The direction of offset from the SCUBA position is the same as that

---

[2]The position uncertainty of SCUBA at 850μm is $\pm3''.2$.

found in Knudsen et al. (2003). However, the low S/N ratio of our observations means that the absolute astrometry of our observations is dominated entirely by phase noise and baseline errors; thus, coordinates with absolute astrometry superior to those describing the optical position cannot be meaningfully derived.

By fitting a Gaussian profile to the observed spectrum, which is taken from the location of the peak emission in the image plane, not from the phase center of the map, we find that the velocity width (FWHM) of the CO(3→2) line of SMM J04135+10277 is 340 ± 120 km s^{-1}. We consider this width uncertain, however, due to a low S/N ratio in the spectral amplitude. The uncertainty in the linewidth was found by plotting Gaussian profiles of varying FWHM over the observed spectrum and choosing which profiles could reasonably be said to fit the line. The integrated flux density over the width of this line, found by adding the flux in the map pixels (excluding any pixels with flux density less than the 1σ value found for the map) in a box centered on, and surrounding, the peak emission and dividing the total by the beam area in pixels, is 5.4 ± 1.3 Jy km s^{-1}. We calculate the uncertainty in the integrated flux, $S_{CO}\Delta V$, using the formula

$$\sigma(S_{CO}\Delta V) = (\sigma_{chan})(\Delta V_{chan})(\sqrt{N_{chan}})(\sqrt{N_{pix,box}/N_{pix,beam}}) \qquad (2)$$

where σ_{chan} is the median single-channel rms per pixel, ΔV_{chan} is the velocity width of a channel, N_{chan} is the number of channels integrated, $N_{pix,box}$ is the number of pixels in the box of integration, and $N_{pix,beam}$ is the beam area in pixels.

Using the relations for L_{CO} and L'_{CO} given in Solomon, Downes, & Radford (1992b), and applying the lensing amplification correction factor of 1.3 (Knudsen et al. 2003) we obtain for SMM J04135+10277 $L_{CO} = 2.2 \times 10^8\, L_\odot$ ($8.8 \times 10^7\, L_\odot$) and $L'_{CO} = 1.7 \times 10^{11}$ K km s^{-1} pc^2 (8.7×10^{10} K km s^{-1} pc^2). Again using Solomon et al. (1992b), with a H$_2$ to CO conversion factor of $\alpha = 0.8\, M_\odot$ (K km s^{-1} pc^2)$^{-1}$, which is the conversion factor Downes & Solomon (1998) find for ULIRGs, we infer a molecular gas mass for SMM J04135+10277 of $M(H_2) = 1.3 \times 10^{11}\, M_\odot$ ($5.3 \times 10^{10}\, M_\odot$). This galaxy is one of the most massive CO systems known to date.

3.1.2.   VCV J140955.5+562827

VCV J140955.5+562827, hereafter referred to as J1409+5628, is a broad-absorption line (BAL) QSO, found in the Second Byurakan Survey (identifier SBS 1408+567) (Chavushyan et al. 1995). It is significantly brighter optically than SMM J04135+10277, with $V = 17.20$ and $B-V = 0.40$, as measured by Stepanian et al. (2001). Korista et al. (1993) derive a redshift of $z = 2.562$ by cross-correlating the QSO's broad emission line spectrum with a

template spectrum (formed by de-redshifting a large sample of BAL spectra by-eye, subtracting a low-order polynomial fit to emission-line free regions, then combining all the spectra to form one high S/N spectrum). J1409+5628 is also a 2MASS point source, with $J = 15.95$, $H = 15.16$, and $K = 14.86$ (Skrutskie et al. 1997). The QSO has recently been detected in 1.2 mm continuum emission by Omont et al. (2003), with $S_{250GHz} = 10.7 \pm 0.6$ mJy. Omont et al. (2003) state that it is one of seven high-z sources with $S_{250GHz} \gtrsim 10$ mJy. There is, however, no indication that the object is strongly lensed, which suggests that the QSO is intrinsically very luminous. A search of the NVSS archive suggests that J1409+5628 is radio-quiet, with a 3σ upper limit of 1.5 mJy at 1.4 GHz (Condon et al. 1998).

Calculating all of our uncertainties in the same way as described in §3.1.1, we detect CO(3→2) emission with significance 5.0σ at 96.462 GHz, corresponding to a redshift of $z_{CO} = 2.585 \pm 0.001$. The spectrum of J1409+5628, taken from the phase center of the map, is shown in Figure 1. By fitting a simple Gaussian line profile, we derive a velocity width (FWHM) of 370 ± 60 km s^{-1}. Figure 3 shows a close-up view of the single COBRA band in which the line is detected, with the fitted line profile displayed.

The map of integrated CO(3→2) emission for J1409+5628 is shown in Figure 2b. The peak of the integrated emission occurs at the phase center of our map, with no other CO sources seen at the same redshift within the primary beam of the telescope. The integrated flux density over the width of the CO line is 2.4 ± 0.7 Jy km s^{-1}. Again using the relations for L_{CO} and L'_{CO} from Solomon et al. (1992b) we obtain for J1409+5628 $L_{CO} = 1.1 \times 10^8 \, L_\odot$ $(4.4 \times 10^7 \, L_\odot)$ and $L'_{CO} = 8.2 \times 10^{10}$ K km s^{-1} pc^2 $(3.3 \times 10^{10}$ K km s^{-1} pc$^2)$. We infer a molecular gas mass for J1409+5628 of $M(\mathrm{H_2}) = 6.6 \times 10^{10} \, M_\odot$ $(2.7 \times 10^{10} \, M_\odot)$. From a direct Gaussian fit to the image plane of the integrated CO map, we place an upper limit to the source size of $6''.3 \times 11''.1$. No significant 3 mm continuum emission is detected from this object, rather we determine a 3σ upper limit of $S_{3mm} < 0.9$ mJy beam^{-1}.

We note that the CO redshift for J1409+5628 is redshifted from the optical, broad-line redshift by $\Delta z = 0.023$. The corresponding discrepancy in velocity space is $\Delta v \sim +1900$ km s^{-1}.

3.1.3. RX J0911.4+0551

RX J0911.4+0551 is a mini-BAL QSO[3], discovered through optical identification of ROSAT All-Sky Survey sources (Bade et al. 1997). The source is gravitationally lensed by an elongated galaxy at $z = 0.769$ (Kneib, Cohen, & Hjorth 2000), which produces the 4 images in an unusual configuration in optical images (Burud et al. 1998). The appearance of the images is thought to be due to a large external shear caused by a massive galaxy cluster, also at $z = 0.769$, at a projected distance of $38''$ (Burud et al. 1998; Kneib et al. 2000). The QSO redshift is $z = 2.800$, found by fitting Gaussian profiles to the neutral hydrogen Lyman-α and the C IV ($\lambda = 1549$ Å) lines of each QSO image, then taking the average of the resulting redshift of each image (Bade et al. 1997). Barvainis & Ivison (2002b) measure large submillimeter flux densities of $S_{850\mu m} = 26.7 \pm 1.4$ mJy and $S_{450\mu m} = 65 \pm 19$ mJy, and infer from these values that the host galaxy is likely to have a significant cold dust component. Barvainis et al. (2002a) attempted, without success, to detect RX J0911.4+0551 in CO(3→2) emission with the IRAM Plateau de Bure interferometer, at the same redshift we adopt in the current observations ($z = 2.807$), but using a more extended configuration and so with higher spatial resolution. They attribute the lack of detection to the combination of uncertainty in the optical redshift and small instrumental bandwidth (560 or 595 MHz, not specifically stated for each source), finding a line rms of 1.2 mJy/100 km s^{-1}. Barvainis et al. (2002a) also report 1 and 3 mm continuum detections for RX J0911.4+0551 of $S_{1mm} = 10.2 \pm 1.8$ mJy beam^{-1} and $S_{3mm} = 1.7 \pm 0.3$ mJy beam^{-1}, which, together with the SCUBA data, fit well the scenario that RX J0911.4+0551 has a significant cold dust component. We note that RX J0911.4+0551 is radio-quiet: the FIRST Survey (White et al. 1997) reports a 1.4 GHz flux density upper limit of 0.45 mJy.

We tentatively detect CO(3→2) emission from RX J0911.4+0551 with a significance of 3.7σ, again calculating all uncertainties as in §3.1.1. The line is centered at 91.088 GHz, which corresponds to a redshift of $z_{CO} = 2.796 \pm 0.001$. We note that the CO redshift of RX J0911.4+0551 turns out to be slightly blueshifted relative to the broad-line redshift, $\Delta v \sim -320$ km s^{-1}, and places the line emission peak just outside the bandwidth of the correlator used by Barvainis et al. (2002a). No other significant CO sources are seen within the array's primary beam; the resolution of our observations is not sufficient to resolve the multiple images of this QSO that one would expect from the lensing model. The integrated CO emission map is shown in Figure 2c, where we see that the peak of the emission is slightly north of the phase center of the observations. From a direct Gaussian fit to this

---

[3]The mini-BAL designation indicates that the velocity spread of the QSO's absorption trough, 3200 km s^{-1}, is just outside the usual velocity range that defines a BAL QSO.

map, we find an upper limit to the source size of $13\rlap{.}''0 \times 6\rlap{.}''9$. The velocity width (FWHM) of the CO line is 350 ± 60 km s^{-1}, and the integrated flux density over this line width is 2.9 ± 1.1 Jy km s^{-1}. Uncorrected for lensing, the integrated flux corresponds to a CO luminosity and molecular gas mass of $L_{CO} = 1.5 \times 10^8\,L_\odot$ ($6.0 \times 10^7\,L_\odot$), $L'_{CO} = 1.1 \times 10^{11}$ K km s^{-1} pc^2 (4.5×10^{10} K km s^{-1} pc^2), and $M(\mathrm{H_2}) = 9.1 \times 10^{10}\,M_\odot$ ($3.6 \times 10^{10}\,M_\odot$), from the relations in Solomon et al. (1992b). Using the lens magnification factor of 21.8 quoted in Barvainis & Ivison (2002b), these quantities decrease to the following: $L_{CO} = 6.9 \times 10^6\,L_\odot$ ($2.8 \times 10^6\,L_\odot$), $L'_{CO} = 5.2 \times 10^9$ K km s^{-1} pc^2 (2.1×10^9 K km s^{-1} pc^2), and $M(\mathrm{H_2}) = 4.2 \times 10^9\,M_\odot$ ($1.7 \times 10^9\,M_\odot$).

We tentatively detect 3 mm continuum emission from RX J0911.4+0551, identifying a $\sim 3\sigma$ source at the phase center of the continuum map with flux density $S_{3mm} = 0.92 \pm 0.29$ mJy beam^{-1}. This value for S_{3mm} differs from Barvainis et al. (2002a) by 0.8 mJy beam^{-1}, thus the values do not formally agree. Our tentative detection may be spurious, however, due to phase offsets and other errors collecting at the phase center of a map.

3.2. Non-Detection: LBQS 0018-0220

LBQS 0018-0220 is a QSO found in the Large, Bright Quasar Survey (LBQS) (Foltz et al. 1989). Hewett, Foltz, & Chaffee (1995) find a broad-line redshift of $z = 2.596 \pm 0.005$, though we searched for CO at the original redshift measurement from Foltz et al. (1989), $z = 2.56$. The LBQS measures a photographic magnitude of $B = 17.4$, but more recently, Richards et al. (1997) report CCD magnitudes of $g^* = 17.20$ and $r^* = 16.95$. LBQS 0018-0220 is also detected by 2MASS (Skrutskie et al. 1997), with measured near-infrared magnitudes of $J = 16.2$ and $H = 15.4$. LBQS 0018-0220 has a narrow absorption line on its Lyman-α line, according to Forster et al. (2001). Priddey et al. (2003a) report a submillimeter flux density of $S_{850\mu m} = 17.2 \pm 2.9$ mJy measured with SCUBA. No radio continuum emission has been observed from this QSO, with 3σ upper limits on flux density of 0.18 mJy at 8.4 GHz (Hooper et al. 1995) and 1.5 mJy at 1.4 GHz (Condon et al. 1998).

We do not detect CO(3→2) emission from LBQS 0018-0220, despite the 4 GHz bandwidth made available by the COBRA correlator, which corresponds to a range of redshift of $2.489 < z < 2.631$. Our observations yield a single-channel rms of 3.3 mJy beam^{-1}, which in turn corresponds to a 3σ-upper limit to the integrated flux density at 97.1 GHz of 1.3 Jy km s^{-1}, assuming a typical line FWHM of 300 km s^{-1} and using equation (2) in §3.1.1. This integrated flux places upper limits to the CO luminosity and molecular gas mass of $L_{CO} < 5.8 \times 10^7\,L_\odot$ ($2.4 \times 10^7\,L_\odot$), $L'_{CO} < 4.4 \times 10^{10}$ K km s^{-1} pc^2 (1.8×10^{10} K km s^{-1} pc^2),

and $M(\mathrm{H}_2) < 3.5 \times 10^{10}\,M_\odot$ $(1.4 \times 10^{10}\,M_\odot)$.

As this work was in revision, it was made known to us that CO(3→2) emission from LBQS 0018-0220 had been detected with the IRAM Plateau de Bure interferometer at the same time, at a level just below the sensitivity limit of our OVRO observations of this object.

3.3. High-z CO Emitters as a Whole

In Table 2, we have summarized the $z > 1$ objects with CO detections published to date, including the results presented here. At least 25 high-redshift objects are known CO emitters, with a number of objects detected in more than one CO transition. At the bottom of the table, the mean and median values of ΔV_{FWHM} and $S_{CO}\Delta V$ are given, for the sample of CO(3→2) detections only as well as the sample of all the objects in the table.

The three detections reported in this paper, for J1409+5628, RX J0911.4+0551, and SMM J04135+10277, have velocity widths and integrated line fluxes that lie within the range set by the $z > 1$ sample of CO detections. With an integrated flux nearly twice the mean of the CO(3→2) sample, SMM J04135+10277 may have the largest lensing-corrected molecular gas mass of any galaxy yet detected, even greater than that of PSS 2322+1944 (with $M(\mathrm{H}_2) = 5.5 \times 10^{10}\,M_\odot$ after using the lensing magnification factor 2.5 from Carilli et al. 2003). The low dust temperature inferred by Knudsen et al. (2003) suggests that not all of the submillimeter emission can be produced by an AGN, and together with the high molecular gas mass, it suggests that this galaxy is undergoing a massive burst of star formation. By contrast, the measurements of integrated flux for J1409+5628 and RX J0911.4+0551 lay close to the median and mean of the CO(3 → 2) detection sample, respectively.

Figure 4 shows a histogram of the redshifts of the objects listed in Table 2, with a bin size of $\Delta z = 0.2$. This diagram represents a graphical summary of the status of the field of high-z CO detection, and is not intended to indicate any statistical trends. Many of the reported detections cluster around $z \sim 2.5$, and one may point out that this clustering appears similar to the distribution of redshifts of submillimeter galaxies (median(z) = 2.4, Chapman et al. 2003). However, that CO detections are most numerous here may not be surprising, given that the most easily observed millimeter band using currrent interferometers is the 3 mm band (85 to 115 GHz), and this band corresponds to CO(3→2) at $z \sim 2 - 3$.

A sample size of just 25 CO emitters is too small to draw any statistically significant conclusions, given the range of redshift and the selection criteria that have been used to identify the sources. Nonetheless, we see from Figure 4 that CO emission can be detected over the entire range of redshift currently observable by available instruments. From the

standpoint of galaxy and QSO co-evolution, this prompts the question of whether CO, and by inference large masses of gas with significant heavy element enrichment, can be detected in all IR-bright quasars, particularly those at high redshift? Of optically selected, IRAS detected, nearby, PG QSOs, a large fraction have CO detections (Alloin et al. 1992; Evans et al. 2001; Scoville et al. 2003).

At high redshift, however, the fraction of known QSOs with CO detections is not high, likely due to limited ranges of redshift that are searched (limited in spectrometer bandwidth and target selection) and large required integration times. However, the growing number of submillimeter QSO detections suggests that there may yet be many more high-z CO sources, since submillimeter flux density is proportional to the intrinsic FIR luminosity and ISM mass of a galaxy. We mention in §1 that the majority of high-z CO detections come from galaxies with $S_{850\mu m} > 10$ mJy. In fact, the 10 brightest submillimeter QSOs with measured redshifts, all with $S_{850\mu m} > 20$ mJy, are CO sources (B1938+666, with $S_{850\mu m} = 35$ mJy from Barvainis & Ivison 2002b, has no published redshift). 30% of high-z QSOs are detected in the millimeter and/or submillimeter continuum and most of those galaxies have CO detections (see Omont et al. 2001; Omont et al. 2003; Priddey et al. 2003a; Priddey et al. 2003b; Isaak et al. 2002). There are at least 20 more QSOs with $z > 1$ in the literature with recently published values of $S_{850\mu m}$ in the range 8-10 mJy in which a CO detection has not been published. If these QSOs are CO sources, not only would they increase significantly the fraction of high-z QSOs with CO detections, but also strengthen the link between the submillimeter galaxy population and the QSO phenomenon and support the scenario of co-evolution of galaxies and massive black holes.

The relative luminosity contributions from star formation and AGN to the large submillimeter emission of high-z QSOs is a related issue of much interest. Yun et al. (2004) suggest that, in the nearby universe, optically selected QSOs are distinct in nature from the ULIRG population even if their host galaxies are rich in molecular gas. They suggest that the presence of large molecular gas reservoirs in QSOs does not necessarily imply a high rate of star formation; thus, the fact that we detect CO in SMM J04135+10277, J1409+5628, and RX J0911.4+0551 does not definitively show that these objects' luminosities are dominated by star formation. We must seek avenues other than CO detection to understand the sources of a galaxy's luminosity. In the case of high-z QSOs, the galaxies are too distant to determine independently if the QSO hosts are undergoing starbursts (e.g. by detecting clumpy, irregular morphology, or by imaging young, super star clusters in the host galaxy). However, the detection of the HCN(1→0) transition in the submillimeter-bright, CO detected, H1413+117 (the Cloverleaf quasar, $z = 2.558$) by Solomon et al. (2003) suggests that at least some high-z IR-bright QSOs experience major star formation activity during their QSO phase, and that a significant part of the FIR emission comes from the star formation

(as opposed to coming from the AGN). To determine if our, and other, submillimeter-bright, molecular gas-rich, high-z QSOs have a high percentage of their FIR luminosity due to star formation, these galaxies should also be searched for HCN emission. However, it may be some time before such an investigation becomes practical, as the recent work of both Solomon et al. (2003) and Isaak, Chandler, & Carilli (2004) imply that only the most luminous HCN sources can be detected at high redshift with currently available instruments. Isaak et al. (2004) suggest that we will have to wait until the EVLA[4] comes on line in order to have the necessary sensitivity to detect HCN in many high-z galaxies.

Finally, while a thorough, systematic evaluation of the range and sense of the relative redshift differences between the QSO and its host galaxy is beyond the scope of this paper, we wish to draw attention to the variation in this offset in Figure 5, which is a plot of the difference between the published optical redshift (representing the QSO redshift) and the CO redshift (representing the host galaxy redshift) in the sense $z_{CO} - z_{optical}$. The need for the large bandwidth of the COBRA correlator at OVRO is apparent in Figure 5, since the range of redshift offsets is large, and it is impossible to know *a priori* how different the host galaxy's redshift will be. The clustering of points (representing CO-detected objects only) about the $z_{CO} - z_{optical} = 0$ line and the relatively small number of outliers likely reflects the bias of the narrow bandwidths used in the past, toward detecting objects with small redshift offsets. Objects searched for CO, but not detected due to unknown redshift offsets, are not included in the plot. Undoubtedly such cases exist and will increase the dispersion in Figure 5. The large increase in spectral bandwidth provided by COBRA will certainly increase the likelihood of actually having a galaxy's CO line fall in the observed spectral window.

4. CONCLUSIONS

Three more high-z QSOs have been detected in CO emission, SMM J04135+10277 at $z = 2.846$, VCV J140955.5+562827 at $z = 2.585$, and RX J0911.4+0551 at $z = 2.796$, using the new COBRA correlator at the Owens Valley Radio Observatory. All three submillimeter-bright QSOs possess large reservoirs of molecular gas, further linking submillimeter galaxies to their QSO contemporaries, and SMM J04135+10277 may be one of the most massive CO systems known.

We thank the anonymous referee for helpful comments to improve this paper. We also

---

REFERENCES

Alloin, D., Barvainis, R., Gordon, M. A., & Antonucci, R. R. J. 1992, A&A, 265, 429

Andreani, P., Cimatti, A., Loinard, L., & Röttgering, H. 2000, A&A, 354, L1

Bade, N., Siebert, J., Lopez, S., Voges, W., & Reimers, D. 1997, A&A, 317, L13

Baker, A. J., Tacconi, L. J., Genzel, R., Lehnert, M. D., & Lutz, D. 2004, ApJ, in press

Barvainis, R., Tacconi, L., Antonucci, R., Alloin, D., & Coleman, P. 1994, Nature, 371, 586

Barvainis, R., Alloin, D., Guilloteau, S., & Antonucci, R. 1998, ApJ, 492, L13

Barvainis, R., Alloin, D., & Bremer, M. 2002, A&A, 385, 399

Barvainis, R., & Ivison, R. 2002, ApJ, 571, 712

Bertoldi, F., et al. 2003, A&A, 406, L55

Bertoldi, F., et al. 2003, A&A, 409, L47

Blain, A. W., Barnard, V. E., & Chapman, S. C. 2003, MNRAS, 338, 733

Burud, I., et al. 1998, ApJ, 501, L5

Carilli, C. L., et al. 2001, ApJ, 555, 625

Carilli, C. L., Lewis, G. F., Djorgovski, S. G., Mahabal, A., Cox, P., Bertoldi, F., & Omont, A. 2003, Science, 300, 773

Chapman, S. C., Blain, A. W., Ivison, R. J., & Smail, I. R. 2003, Nature, 422, 695

Chavushyan, V. O., Stepanian, J. A., Balayan, S. K., & Vlasyuk, V. V. 1995, AstL, 21, 804

Condon, J. J., Cotton, W. D., Greisen, E. W., Yin, Q. F., Perley, R. A., Taylor, G. B., & Broderick, J. J. 1998, AJ, 115, 1693

Cowie, L. L., Barger, A. J., & Kneib, J.–P. 2002, AJ, 123, 2197

Cox, P., et al. 2002, A&A, 387, 40

De Breuck, C., et al. 2003, A&A, 401, 911

De Breuck, C., Neri, R., & Omont, A. 2003, New Astron. Rev., 47, 285

Dey, A., Graham, J. R., Ivison, R. J., Smail, I., Wright, G. S., & Liu, M. C. 1999, ApJ, 519, 610

Downes, D., Solomon, P. M., & Radford, S. J. E. 1995, ApJ, 453, L65

Downes, D., & Solomon, P. M. 1998, ApJ, 507, 615

Downes, D., Neri, R., Wiklind, T., Wilner, D. J., & Shaver, P. A. 1999, ApJ, 513, L1

Evans, A. S., Frayer, D. T., Surace, J. A., & Sanders, D. B. 2001, AJ, 121, 1893

Ferrarese, L., & Merritt, D. ApJ, 539, L9

Foltz, C. B., Chaffee, F. H., Hewett, P. C., Weymann, R. J., Anderson, S. F., & MacAlpine, G. M. 1989, AJ, 98, 1959

Forster, K., Green, P. J., Aldcroft, T. L., Vestergaard, M., Foltz, C. B., & Hewett, P. C. 2001, ApJS, 134, 35

Frayer, D. T., et al. 1998, ApJ, 506, L7

Frayer, D. T., et al. 1999, ApJ, 514, L13

Gebhardt, K., et al. 2000, ApJ, 539, L13

Guilloteau, S., Omont, A., McMahon, R. G., Cox, P., & Petitjean, P. 1997, A&A, 328, L1

Guilloteau, S., Omont, A., Cox, P., McMahon, R. G., & Petitjean, P. 1999, A&A, 349, 363

Hewett, P. C., Foltz, C. B., & Chaffee, F. H. 1995, AJ, 109, 1498

Holland, W. S., et al. 1999, MNRAS, 303, 659

Hooper, E. J., Impey, C. D., Foltz, C. B., and Hewett, P. C. 1995, ApJ, 445, 62

Irwin, M. J., Ibata, R. A., Lewis, G. F., & Totten, E. J. 1998, ApJ, 505, 529

Isaak, K. G., Priddey, R. S., McMahon, R. G., Omont, A., Peroux, C., Sharp, R. G., & Withington, S. 2002, MNRAS, 329, 149

Isaak, K. G., Chandler, C. J., & Carilli, C. L. 2004, MNRAS, 348, 1035

Ivison, R. J., et al. 1998, MNRAS, 298, 583

Ivison, R. J., et al. 2002, MNRAS, 337, 1

Kneib, J.–P., Mellier, Y., Fort, B., & Mathez, G. 1993, A&A, 273, 367

Kneib, J.–P., Cohen, J. G., & Hjorth, J. 2000, ApJ, 544, L35

Knudsen, K. K., van der Werf, P. P., & Jaffe, W. 2003, A&A, 411,343

Korista, K. T., Voit, G. M., Morris, S. L., & Weymann, R. J. 1993, ApJS, 88, 357

Lewis, G. F., Chapman, S. C., Ibata, R. A., Irwin, M. J., & Totten, E. J. 1998, ApJ, 505, L1

McMahon, R. G., Priddey, R. S., Omont, A., Snellen, I., & Withington, S. 1999, MNRAS, 309, L1

Neri, R., et al. 2003, ApJ, 597, L113

Omont, A., Petitjean, P., Guilloteau, S., McMahon, R. G., Solomon, P. M., & Pecontal, E. 1996, Nature, 382, 428

Omont, A., Cox, P., Bertoldi, F., McMahon, R. G., Carilli, C., & Isaak, K. G. 2001, A&A, 374, 371

Omont, A., et al. 2003, A&A, 398, 857

Papadopoulos, P., Röttgering, H., van der Werf, P. P., Guilloteau, S., Omont, A., van Breugel, W. J. M., & Tilanus, R. 2000, ApJ, 528, 626

Planesas, P., Martin-Pintado, J., Neri, R., & Colina, L. 1999, Science, 286, 2493

Priddey, R. S., Isaak, K. G., McMahon, R. G., & Omont, A. 2003a, MNRAS, 339, 1183

Priddey, R. S., Isaak, K. G., McMahon, R. G., Robson, E. I., & Pearson, C. P. 2003b, MNRAS, 344, 74

Richards, G. T., Yanny, B., Annis, J., Newberg, H. J. M., McKay, T. A., York, D. G., & Fan, X. 1997, PASP, 109, 39

Robson, E. I., et al. 2004, MNRAS, submitted

Rowan–Robinson, M., et al. 1993, MNRAS, 261, 513

Sault, R. J., Teuben, P. J., & Wright, M. C. H. 1995, in ASP Conf. Ser. 77, Astronomical Data Analysis Software and Systems IV, ed. R. A. Shaw, H. E. Payne, & J. J. E. Hayes (San Francisco: ASP), 433

Scoville, N. Z., Carlstrom, J. E., Chandler, C. J., Phillips, J. A., Scott, S. L., Tilanus, R. P. J., & Wang, Z. 1993, PASP, 105, 1482

Scoville, N. Z., Yun, M. S., Windhorst, R. A., Keel, W. C., & Armus, L. 1997, ApJ, 485, L21

Scoville, N. Z., Frayer, D. T., Schinnerer, E., & Christopher, M. 2003, ApJ, 585, L105

Skrutskie, M. F., et al. 1997, Proc. Workshop "The Impact of Large Scale Near-IR Sky Surveys", ed. Garzón, F. et al. (Dordrecht: Kluwer), 25

Smail, I., Ivison, R. J., & Blain, A. W. 1997, ApJ, 490, L5

Smail, I., Ivison, R. J., Blain, A. W., & Kneib, J.–P. 1998, ApJ, 507, L21

Smail, I., Ivison, R. J., Blain, A. W., & Kneib, J.–P. 2002, MNRAS, 331, 495

Smail, I., Ivison, R. J., Gilbank, D. G., Dunlop, J. S., Keel, W. C., Motohara, K., & Stevens, J. A. 2003, ApJ, 583, 551

Solomon, P. M., Downes, D., & Radford, S. J. E. 1992a, Nature, 356, 318

Solomon, P. M., Downes, D., & Radford, S. J. E. 1992b, ApJ, 398, L29

Solomon, P., Vanden Bout, P., Carilli, C., & Guelin, M. 2003, Nature, 426, 636

Stepanian, J. A., Green, R. F., Foltz, C. B., Chaffee, F., Chavushyan, V. H., Lipovetsky, V. A., & Erastova, L. K. 2001, AJ, 122, 3361

Tytler, D., & Fan, X. 1992, ApJS, 79, 1

Walter, F., et al. 2003, Nature, 424, 406

White, R. L., Becker, R. H., Helfand, D. J., & Gregg. M. D. 1997, ApJ, 475, 479

Yun, M. S., & Carilli, C. L. 2002, ApJ, 568, 88

Yun, M. S., Reddy, N. A., Scoville, N. Z., Frayer, D. T., Robson, E. I., & Tilanus, R. P. J. 2004, ApJ, 601, 723

Table 1.   Observational Parameters of Sub-mm Bright QSOs

Source	R.A.[a] (J2000.0)	Declination[a] (J2000.0)	Redshift	M_B	$S_{850\mu m}$ (mJy)	Frequency (GHz)	Beam Size[b] ($'' \times ''$)	t_{int}[c] (hours)	Calibrator
LBQS 0018-0220	00 21 27.30	−02 03 33.0	2.560	−28.6	17	97.13	13 × 11	10	0006−063
SMM J04135+10277	04 13 27.50	+10 27 40.3	2.855	· · ·	25	89.70	15 × 11	26	0433+053
RX J0911.4+0551	09 11 27.50	+05 50 52.0	2.807	· · ·	27	90.83	14 × 10	29	0854+201
VCV J140955.5+562827	14 09 55.50	+56 28 27.0	2.560	−28.4	11[d]	97.13	14 × 10	28	1419+543

Note. — Units of right ascension are hours, minutes, and seconds. Units of declination are degrees, arcminutes, and arcseconds.

[a]Optical QSO position.

[b]Theoretical FWHM of OVRO beam at source declination and observed frequency, assuming natural weighting.

[c]Total effective on-source integration time with six telescopes.

[d]1.2 mm flux density, as 850μm flux density has not been measured.

Table 2.   High-z CO Detections Published To Date

Source	Type[a]	z_{CO}	$S_{850\mu m}$ (mJy)	Transition	ΔV_{FWHM} (km s^{-1})	$S_{CO}\Delta V$ (Jy km s^{-1})	Reference
0957+561	QSO	1.414	7.5	CO(2→1)	440	1.2	1,2
HR 10	ERO	1.439	4.9	CO(2→1)	400	1.4	3,4
F 10214+4724	QSO/ULIRG	2.285	50	CO(3→2)	230	4.8	5,6
SMM J16358+4057	Submm	2.385	8.2	CO(3→2)	840	2.3	7,8
53W002	RG	2.394	3.1	CO(3→2)	540	1.5	9,10
SMM J04431+0210	Submm	2.509	7.2	CO(3→2)	350	1.4	7,11
H 1413+117	QSO	2.558	66	CO(3→2)	330	9.9	12,2
SMM J14011+0252	Submm	2.565	6	CO(3→2)	200	2.4	13,14
VCV J1409+5628	**QSO**	**2.585**	$\cdots$	**CO(3→2)**	**370**	**2.4**	**(this paper)**
MG 0414+0534	QSO	2.639	25	CO(3→2)	580	2.6	15,2
MS 1512-cB58	LyB	2.727	4.2	CO(3→2)	170	0.4	16
LBQS 1230+1627B	QSO	2.735	29	CO(3→2)	$\cdots$	0.8	17
RX J0911.4+0551	**QSO**	**2.796**	**27**	**CO(3→2)**	**350**	**2.9**	**(this paper)**
SMM J02399-0136	QSO/Submm	2.808	25	CO(3→2)	710	3.0	18,19
SMM J04135+10277	**QSO/Submm**	**2.846**	**25**	**CO(3→2)**	**340**	**5.4**	**(this paper)**
B3 J2330+3927[b]	RG	3.094	14	CO(4→3)	220	1.3	31
MG 0751+2716	QSO	3.208	26	CO(4→3)	390	6.0	20,2
SMM J09431+4700	Submm	3.346	10.5	CO(4→3)	420	1.1	7,21
TN J0121+1320[b]	RG	3.520	$\cdots$	CO(4→3)	300	1.2	32
6C1909+722	RG	3.532	14	CO(4→3)	530	1.6	22
4C 60.07	RG	3.791	11	CO(4→3)	550	2.5	22
APM 08279+5255	QSO	3.911	75	CO(4→3)	400	3.7	23,24
PSS 2322+1944	QSO	4.120	23	CO(4→3)	375	4.2	25,26
BR 1335-0414	QSO	4.407	14	CO(5→4)	420	2.8	27,28
BR 0952-0115	QSO	4.434	13	CO(5→4)	230	0.9	17,2
BR 1202-0725	QSO	4.690	42	CO(5→4)	320	2.4	29,28
SDSS 1148+5251	QSO	6.419	$\cdots$	CO(3→2)	380	0.2	30
Mean CO(3→2)					**415**	**2.9**	
Median CO(3→2)					**350**	**2.4**	
Mean (all)					**399**	**2.6**	
Median (all)					**380**	**2.4**	

[a]Key to abbreviations – QSO = quasi-stellar object; ERO = extremely red object; ULIRG = ultraluminous infrared galaxy; Submm = submillimeter galaxy; RG = radio galaxy; LyB = Lyman break galaxy

[b]Added in proofs.

References. — (1) Planesas et al. 1999; (2) Barvainis & Ivison 2002; (3) Andreani et al. 2000; (4) Dey et al. 1999; (5) Solomon, Downes, & Radford 1992a and Downes, Solomon, & Radford 1995; (6) Rowan–Robinson et al. 1993; (7) Neri et al. 2003; (8) Ivison et al. 2002; (9) Scoville et al. 1997; (10) Smail et al. 2003; (11) Smail et al. 1997 and Smail et al. 2002; (12) Barvainis et al. 1994; (13) Frayer et al. 1999; (14) Smail et al. 1998; (15) Barvainis et al. 1998; (16) Baker et al. 2004; (17) Guilloteau et al. 1999; (18) Frayer et al. 1998; (19) Ivison et al. 1998; (20) Barvainis et al. 2002a; (21) Cowie et al. 2002; (22) Papadopoulos et al. 2000; (23) Downes et al. 1999; (24) Lewis et al. 1998; (25) Cox et al. 2002; (26) Isaak et al. 2002; (27) Guilloteau et al. 1997; (28) quoted in McMahon et al. 1999; (29) Omont et al. 1996; (30) Walter et al. 2003; (31) De Breuck et al. 2003a; (32) De Breuck, Neri, & Omont 2003b
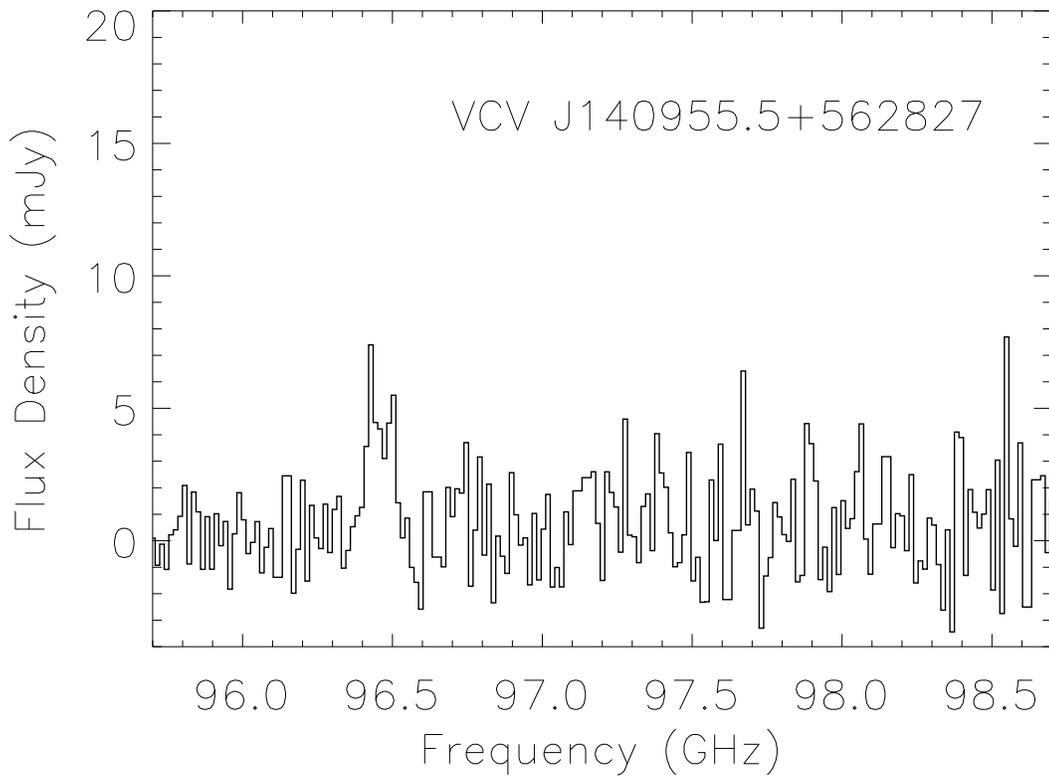
Fig. 1.— Example spectrum from COBRA correlator, showing 3 GHz of the available 4 GHz bandwidth.
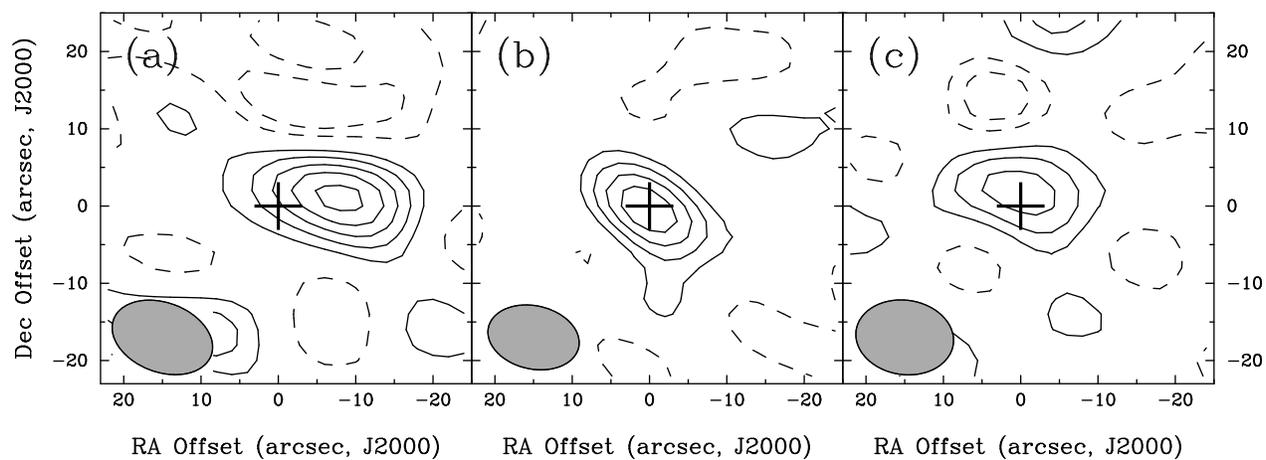
Fig. 2.— Maps of integrated CO emission in (a) SMM J04135+10277, (b) J1409+5628, and (c) RX J0911.4+0551. The contours are multiples (-2,-1,1,2,3,4,5) of the rms noise levels, which are 0.92 Jy beam^{-1} km s^{-1}, 0.49 Jy beam^{-1} km s^{-1}, and 0.88 Jy beam^{-1} km s^{-1}. The crosses mark the phase center in each map. North is up, west is to the right.
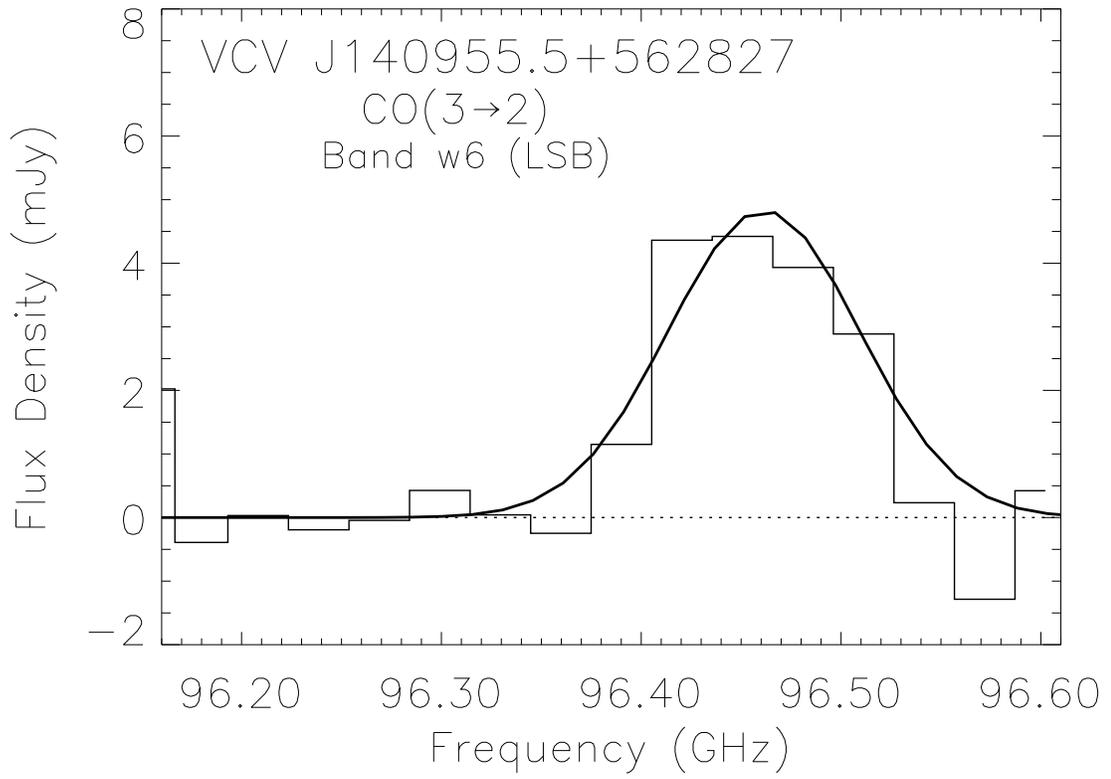
Fig. 3.— Spectral line fit for J1409+5628. The spectrum has been continuum-subtracted and smoothed to a resolution of 97 km s^{-1}.
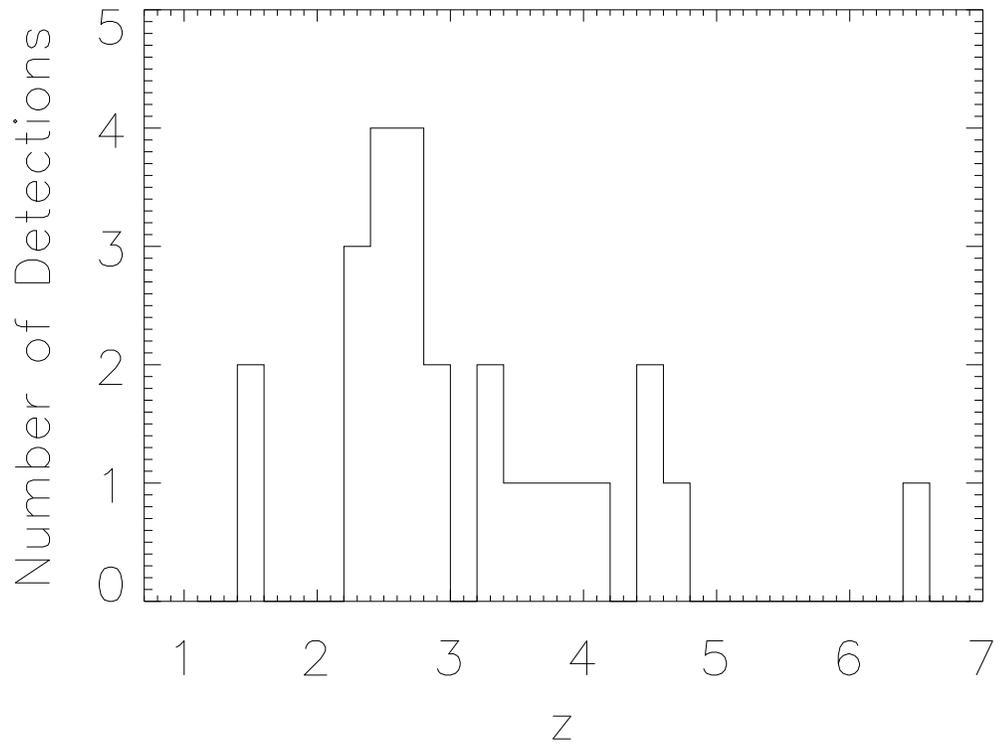
Fig. 4.— Histogram of redshifts of high-z CO detections.
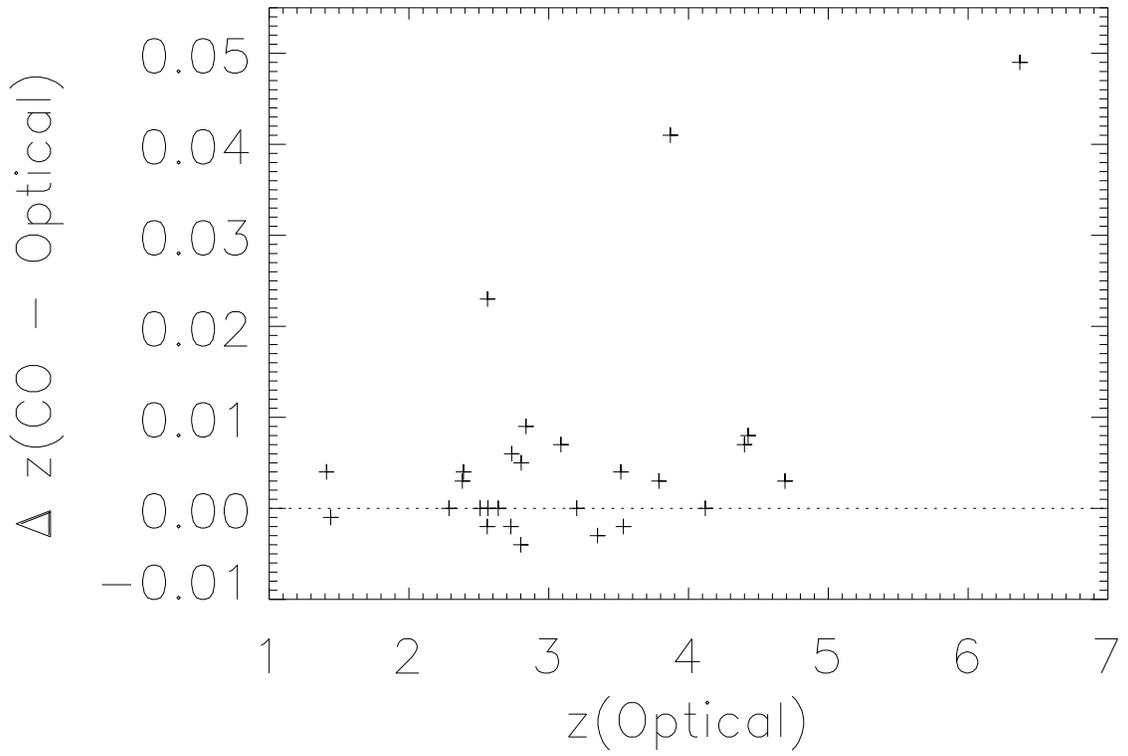
Fig. 5.— Comparison of optical and CO redshifts for high-z CO sources.